

Heat Transfer Analysis Of Nano-fluid Flow In A Converging Nozzle With Different Aspect Ratios

T. Sathish

Research Scholar, Department of Mechanical Engineering, St. Peter's University, Chennai, Tamilnadu, India

Received: June 25, 2017, Accepted: July 27, 2017, Available online: September 12, 2017

Abstract: The study evaluates the nanofluid using finite element analysis with base fluid (water) and seeding particles (Aluminum oxide). This is placed over a convergence channel consisting of varying aspect ratio that are evaluated quantitatively to enhance the heat transfer properties of the nanofluid. We have considered frictional loss characteristics that increases the flow of the fluid with Reynolds numbers varying from 100-2000 is compared. A baseline modeling is established using the methodology analysis for the fluid flow over a rectangular chamber that is designed in the form of a square duct of ratio 1:1. The analysis is carried out over the heat transfer and flow rate characteristics of the nanofluid that converges into the square ducts with different aspect ratio, is analyzed. The concentration of the nano fluid is maintained at the constant rate, which is used for studying the flow rate influence over different aspect ratios. The thermal and flow characteristics is analyzed in such situation and validated against other literatures to check the efficiency in the converging rectangular oxygen free copper channel. The simulation results shows an increase in temperature on the duct out and drop in temperature on the inlet walls of the tube. The pressure changes and shear stress along the walls of the chamber is not much noticed and it is constant throughout the entire chamber.

Keywords: Nanofluid, heat transfer, flow rate, converging nozzle

1. INTRODUCTION

Nanofluids are the new class fluids suspended as a nanosized particles and this forms the base fluid of size 1–100nm. In addition, nanofluid properties make it suitable for potential applications like heat transfer applications and enhancing the thermal conductivity with increased convective heat transfer coefficient than baseline fluid. The nanofluids are considered as single phase fluids while the analysis is carried out to estimate the computational fluid dynamics (CFD). Classical theory concludes that physical properties of nanofluids are considered as functional properties of constituents and concentrations.

Recently, research on nanofluid is treated as a superior heat transfer agent, e.g. coolant in engines. Several literature reported that nanofluids can act as heat transfer agent in rectangular channels with varying aspect ratio. However, researches on converging channels is unavailable, hence, the present work concentrates on flow rate and heat transfer characteristics of convergence channel.

The contribution of work involves nanofluid application on water as base fluid and Aluminium oxide as seeding particle. This

is made to converge in a channel with different aspect ratios. The fluids are evaluated quantitatively to enhance heat transfer characteristics. The frictional loss of nanofluids is increased with Reynolds numbers between 100 - 2000.

Initially, baseline model is considered with water flow over a rectangular channel. The design looks like a square duct chamber with an aspect ratio of 1:1. The heat transfer rate and flow rate characteristics of baseline fluid and nanofluid is carried out in a converging rectangular channel with varying aspect ratio. The concentration of nanofluid is maintained at a constant rate to study the characteristics of fluid with varying Reynolds number.

The remaining section of the paper is mentioned as follows: Section 2 provides the literature survey. Section 3 provides the design of proposed laminar flow inside tubular model. Section 4 provides the simulation and discussions on nanofluid mixture and section 5 concludes the paper.

2. LITERATURE SURVEY

Shah and London (1978) used laminar flow and heat transfer in single phase fluid in flat tube. Park and Pak (2002) used laminar flow in flat tube of various shape and dimension to analyse the

*To whom correspondence should be addressed: Email: sathish.sailer@gmail.com

mixture of ethylene glycol and water. Yang et al. (2005) used laminar heat transfer with graphite nanoparticle. Akbarinia and Behzadmehr (2007) used curved tube with mixed laminar convection. Vajjha et al. (2009) analysed the thermal conductivity of nanofluid mixtures with aluminum oxide, copper oxide and zinc oxide dispersed in base fluid of 60:40 ethylene glycol and water mixture. Bianco et al. (2009) used forced convection circular tube and developed laminar forced convection flow with Al_2O_3 /water nanofluid. Nassan et al. (2010) used square cross-section duct to study the Al_2O_3 /water with CuO /water nanofluids. Huminic et al. (2010) used thermosyphon heat pipe to study the iron oxide nanoparticles. Paul et al. (2010) reviewed on techniques to measure the thermal conductivity of nanofluids and Mohammed et al (2011) reviewed on micro-channels to study the convective heat transfer using nanofluid.

Raveshi et al. (2012) investigated the pool boiling heat transfer enhancement in aluminum water ethylene glycol nanofluids. Peyghambarzadeh et al. (2011) studied the cooling performance of Al_2O_3 /water nanofluid. Kamyar et al. (2012) studied CFD of the nanofluids to evaluate the heat transfer enhancement. Huminic et al. (2012) used heat exchanger to study the flow of nanofluids. Suresh et al. (2012) used straight circular duct fitted with helical screw tape to compare the thermal characteristics of Al_2O_3 /water and CuO /water nanofluids. Mohammed et al (2013) used double pipe heat exchanger with louvered strip inserts to study the heat enhancement of nanofluid.

3. COMPUTATIONAL METHODOLOGY

A nanofluid with Al_2O_3 nano particles of size 50 nm is used to

Table 1. Settings for Ansys Mesher tool for mesh creation

Size	
Advanced Size function	Curvature
Relevance center	medium
Initial size seed	Active assembly
Smoothing	medium
Transition	slow
Span angle center	fine
Curvature Normal Angle	Default (18)
Min size	$1e^{-3}$ m
max face size	$1e^{-3}$ m
Max Size	$1e^{-3}$ m
Growth Rate	1
Min Edge length	$1e^{-2}$ m
Inflation	
Use Automation Inflation	All faces in chosen named selection
Named selection	w-wall
Inflation	First Layer Thickness
First layer height	$1e^{-4}$ m
Max layers	5
Growth Rate	1.2
Inflation Algorithm	Pre
View Advanced Options	No
Patch Conforming Options	
Triangle Surface Mesher	Advancing Front

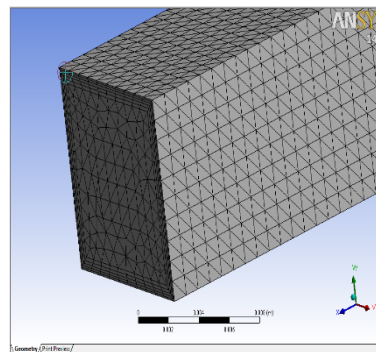


Figure 1. Meshed computational domain

analyse the forced laminar convective heat transfer coefficient, flowing over a horizontal tube. The single phase model is used for carrying out numerical simulation with temperature dependent properties. The numerical simulation is carried out to find nanofluid transport phenomena of diameter <10 nm. Heat transfer theory is used to find the thermal conductivity and the convective heat transfer coefficient, which is directly proportional to the thermal conductivity. The mesh generation over the nano particles is regarded as the critical aspects in simulation. The table.1 shows the mesh creation settings in the computational domain and Fig.1 shows the cross sectional area of the square mesh and tetrahedral elements. To capture the flow at near wall, an inflation layer or the boundary layer is created effectively.

The physical properties of water and Al_2O_3 nano particles is shown in table.2. The nano particles are made to disperse in base fluid and concentration of nano particles are made uniform over the domain. The constituent properties and their concentrations with physical properties is studied for the two phase fluid. The boundary layer profile is shown in Fig.2.

3.1. Numerical Method

The convergence solutions are used in present study to carry out the simulation. The residual results in iterative process, shown in Eq.(1)– Eq.(3) is lower than 10^{-6} . The velocity components V_x , V_y , V_z , temperature T and pressure P are solved using computational domain. The post-processing results in computation of bulk fluid temperature, skin friction coefficient, wall shear stress and convective heat transfer coefficient. The flow rate and heat transfer characteristics of the nanofluid flow is calculated as:

$$\text{Mass: } (\nabla \cdot V) = 0 \quad (1)$$

Table 2. Physical Properties of fluid taken for study

	Water		Al_2O_3 nano particles	
Molar mass	18.02	$[\text{kg.k mol}^{-1}]$	18.02	$[\text{kg.k mol}^{-1}]$
Density	997.0	kg.m^{-3}	1104.2	kg.m^{-3}
Specific heat capacity	4181.7	$\text{J.kg}^{-1}.\text{k}^{-1}$	3317.8	$\text{J.kg}^{-1}.\text{k}^{-1}$
Reference conditions	25°C @ 1 atm pressure		25°C @ 1 atm pressure	
Dynamic viscosity	$8.899E^{-4}$	$\text{kg.m}^{-1}.\text{s}^{-1}$	9.5575-4	$\text{kg.m}^{-1}.\text{s}^{-1}$
Thermal conductivity	0.6069	$\text{w.m}^{-1}.\text{k}^{-1}$	0.5129	$\text{w.m}^{-1}.\text{k}^{-1}$

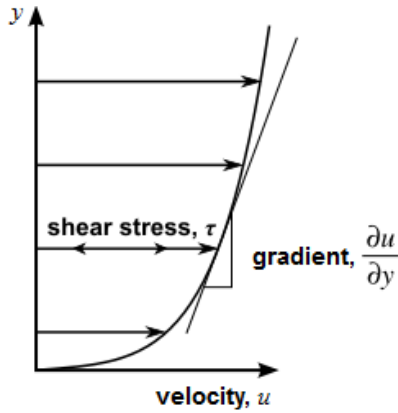


Figure 2. Boundary layer profile of a moving fluid

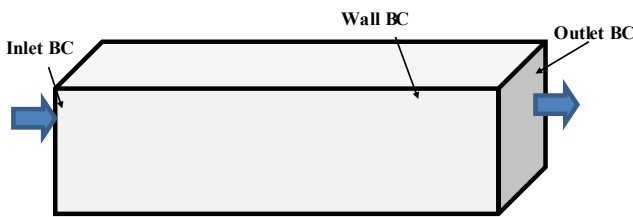


Figure 3. Boundary surface for CFD analysis

$$\text{Momentum: } \rho_{nf} (\nabla \cdot V) V = -\nabla P + \mu_{nf} \nabla^2 V \quad (2)$$

$$\text{Energy: } \rho_{nf} C_{nf} (\nabla \cdot V) T = k_{nf} \nabla^2 T \quad (3)$$

3.2. Boundary Conditions

The nonlinear coupled system is formed using mass, momentum and energy that is subjected to boundary conditions. At flat tube inlet surface, the velocity and temperature is predefined. The velocity is determined using Reynolds number inside chamber that carries nanofluid at a temperature of 90°C (363 K). The axial velocity is made uniform at the inlet chamber, which results in ideal flow pattern. This is carried out, since non-uniformities may arise when the fluid enters the inlet. In outlet section, the outflow boundary condition is selected under thermal entry length $X_T = 0.05Re'Pr'Dh < \text{tubelength}$. During Fluent, the outlet condition is similar to full temperature and velocity profile with axial derivatives = 0. However, the flow is not developed for higher Reynolds number. Under such conditions, pressure outlet boundary condition is adopted. All along the tube wall, no-slip boundary condition is imposed for velocity. The Fig.3 shows the boundary surfaces, where the inlet surface is the entry face for nanofluid and outlet face is the exit face of fluid.

The aspect ratio of channel is defined as the ratio between inlet channel area and outlet channel area. The aspect ratio used in present study is shown in table.3 and the height of the channel outlet is varied in order to accommodate varying outlet channel area. The inlet velocity is used to vary the inflow rate of channel, calculated

using Reynolds number. Table.4 shows four Reynolds numbers for testing the nano fluid.

4. RESULTS AND DISCUSSION

The analysis on nanofluid is carried with water flow as baseline case. This is tested on a rectangular or square duct chamber with an aspect ratio of 1:1. The test like flow rate and heat transfer characteristics is carried out to find the concentration of nanofluid under the influence of varying Reynolds number. Finally, the flow rate with thermal characteristics of rectangular oxygen free copper channel is studied using finite element analysis.

4.1. Water Nanofluid Flow in a 1:1 Channel without Convergence (AR = 1.0 & Re = 2000)

The results are analysed using water-nanofluid, which is flowing inside the rectangular channel at an aspect ratio of 1:1. The static pressure contours over convergence chamber walls is shown in Fig.4 in a computational domain. In order to maintain continuity, channel inlet pressure is made higher and the inlet pressure is updated at solver. The entire domain is shown in Fig.5(a) and close inlet and outlet view is shown in Fig.5(b) and Fig.5(c). The wall shear stress contours over rectangular channel walls with an aspect ratio = 1 is thus evaluated. The wall temperature contour of computational domain wall with aspect ratio on square duct of 1 is shown in Fig.6. The inlet contour (Fig.6(b)) in convergence wall consists of thermal gradients and has boundary layer formation.

4.2. Water Flow in a Channel with Convergence (AR = 2.0 & Re = 2000)

The analysis of CFD in a convergence square duct chamber with ratio 2 has an external heat transfer coefficient of 50 W/m²-K. Fig.7 shows the simulated view of contours on convergence wall chamber. It is seen that the pressure is unaltered and it is closer to the channel without any heat transfer. In both cases, it is found that the drop in pressure over the channel is similar. The contours of temperature on channel wall is shown in Fig.8. The walls are cooled due to convective heat loss of heat coefficient (50 W/m²K). The hot water flowing inside the duct is found to lose its heat and shear stress contours at the wall along axial direction is shown in Fig.9.

The variation of wall temperature with Reynolds number is shown in Fig.10, over different aspect ratios. The wall temperature of channel increases rapidly as the flow increases with a constant

Table 3. Channel Aspect ratio

Inlet Area (mm ²)	Outlet Height (mm)	Out Area (mm ²)	Area Ratio AR = inlet/outlet
100	10	100	1.00
100	9	90	1.11
100	8	80	1.25
100	7	70	1.43
100	6	60	1.67
100	5	50	2.00

Table.4. Inlet diameter with Reynolds number

Reynolds number	Inlet Velocity (m/s)
100	0.00866
500	0.04328
1000	0.08656
2000	0.17311

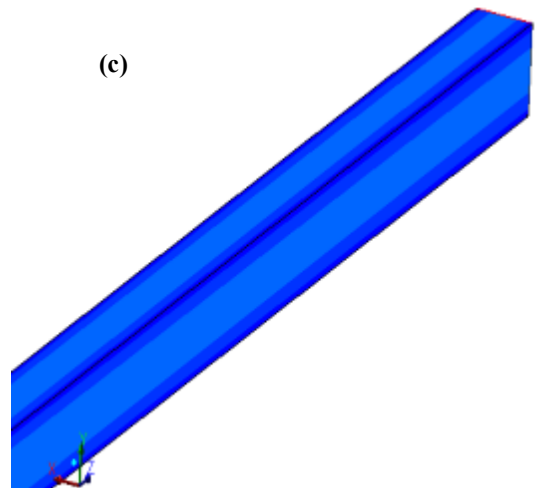
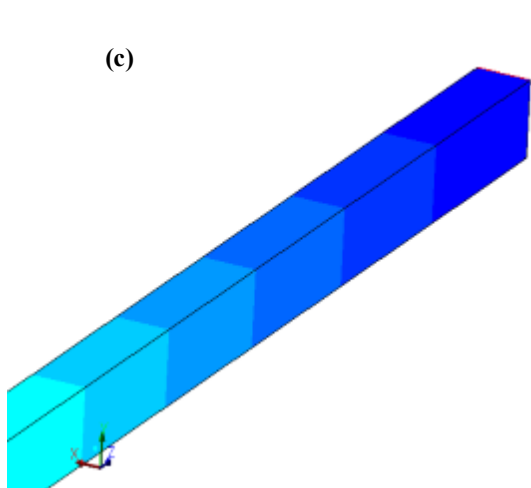
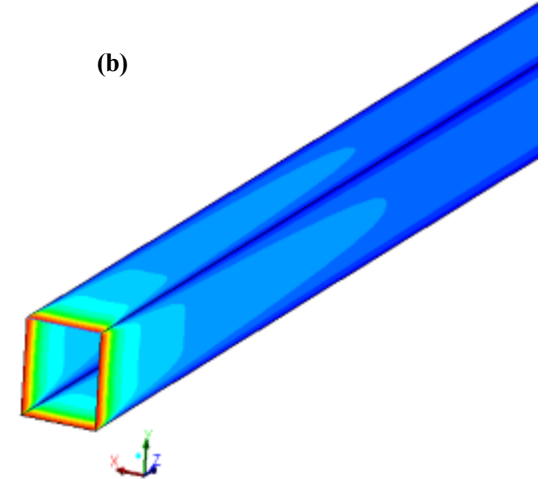
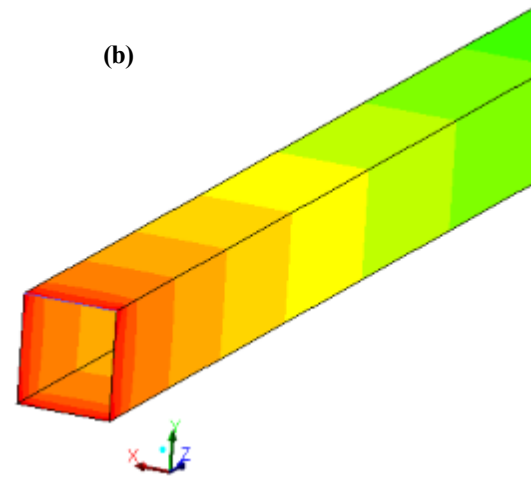
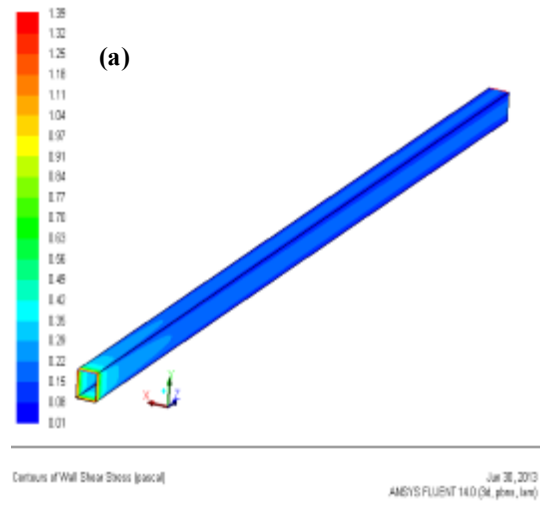
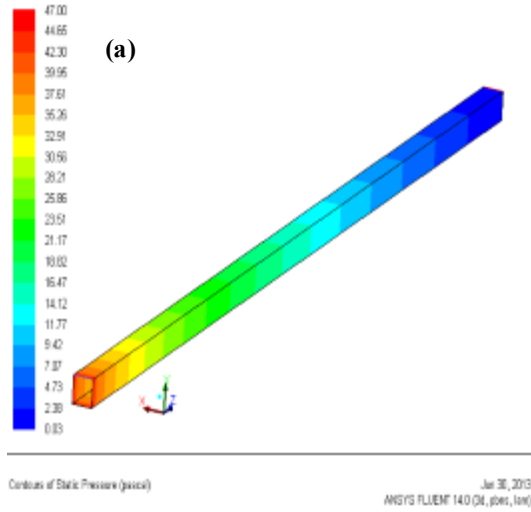
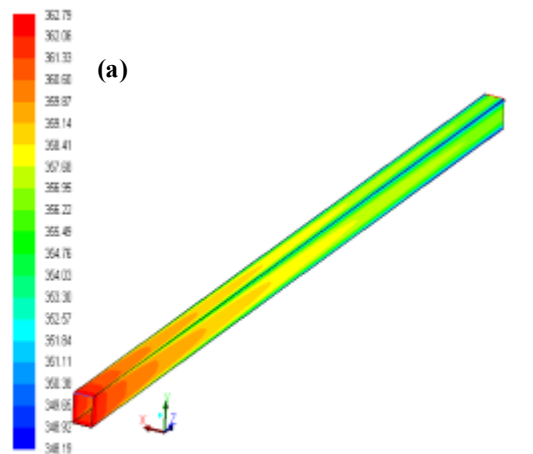
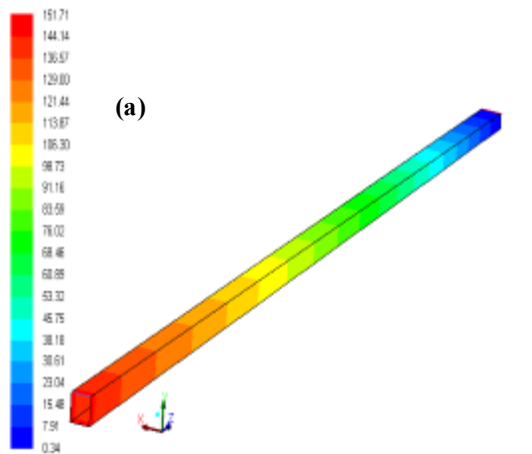


Figure 4. Contours of static pressure on 1:1 channel (AR = 1.0 & Re = 2000)

Figure 5. Contours of wall shear stress on 1:1 channel (AR = 1.0 & Re = 2000)



Contours of Static Temperature (K) ANSYS FLUENT 14.0 (64_bit, linux) Jun 30, 2013



Contours of Static Pressure (pascal) ANSYS FLUENT 14.0 (64_bit, linux) Jun 30, 2013

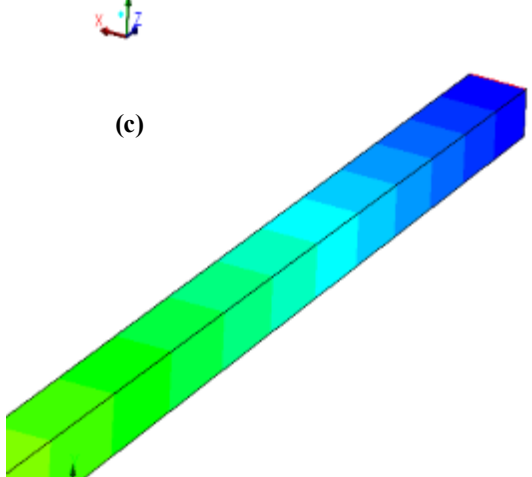
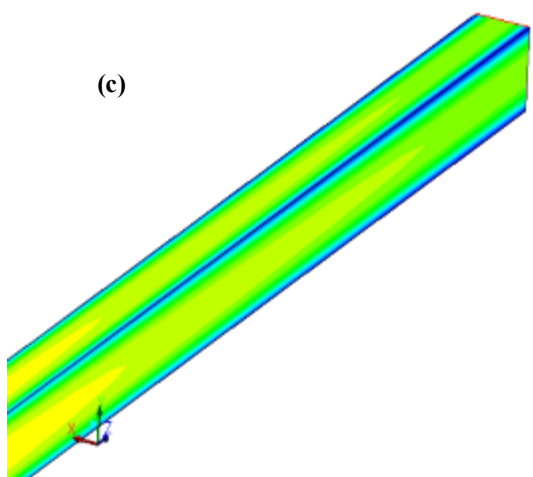
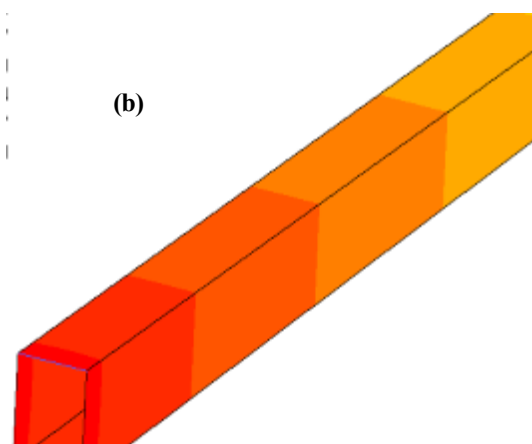
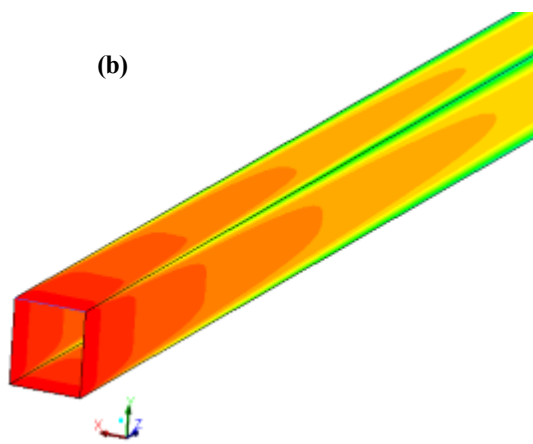


Figure 6. Contours of wall temperature on a 1:1 channel (AR = 1.0 & Re = 2000)

Figure 7. Contours of static pressure on converged channel (AR=2.0)

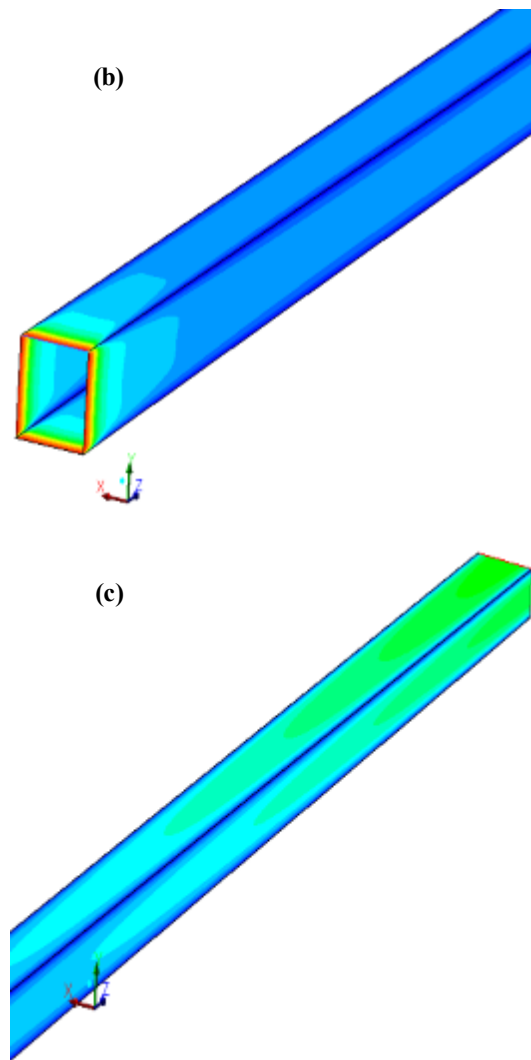
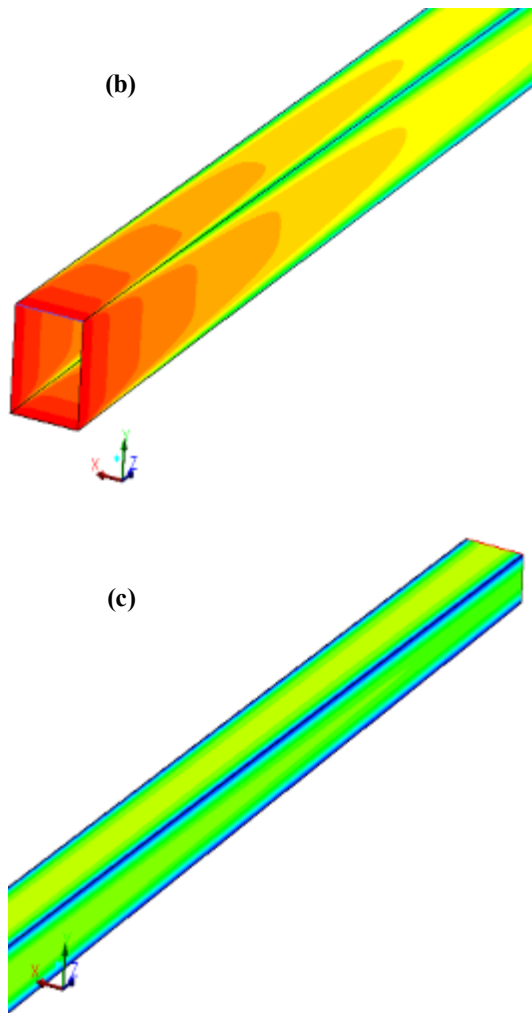
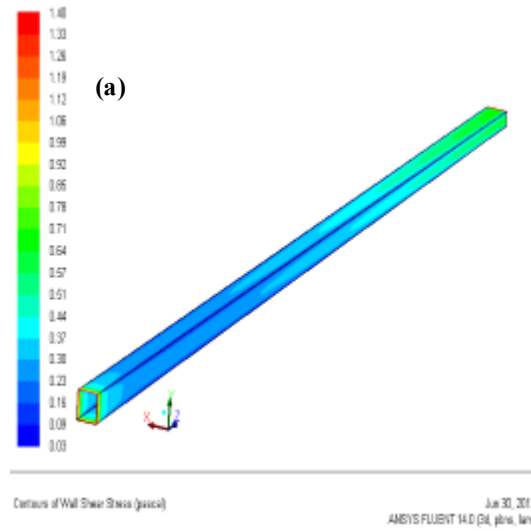
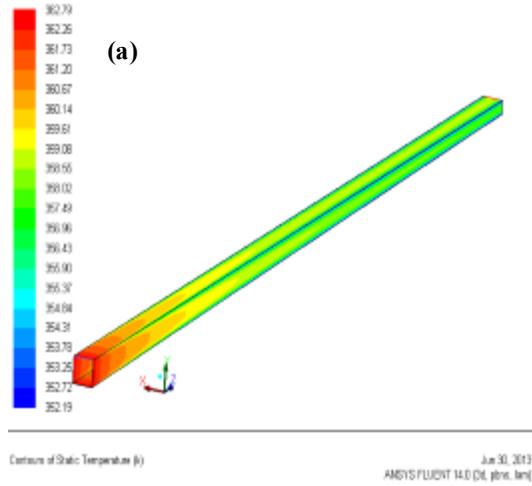


Figure 8. Contours of wall temperature on converged channel (AR=2.0)

Figure 9. Contours of wall shear stress (AR=2.0)

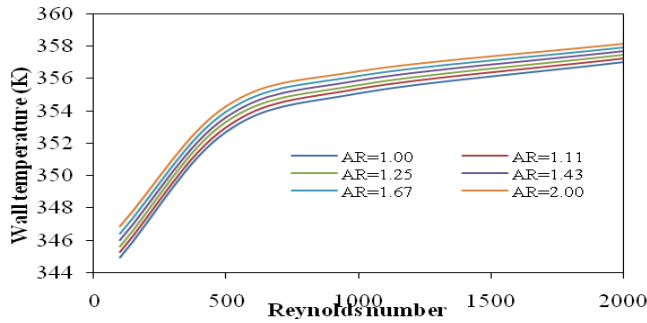


Figure 10. Wall temperature variation with Reynolds number

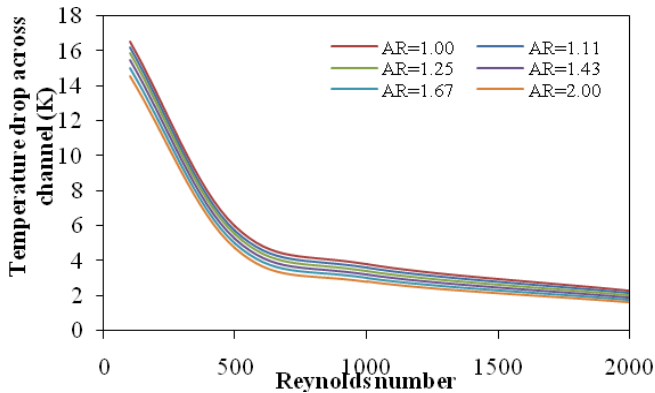


Figure 11. Temperature drop variation across the duct with Reynolds number

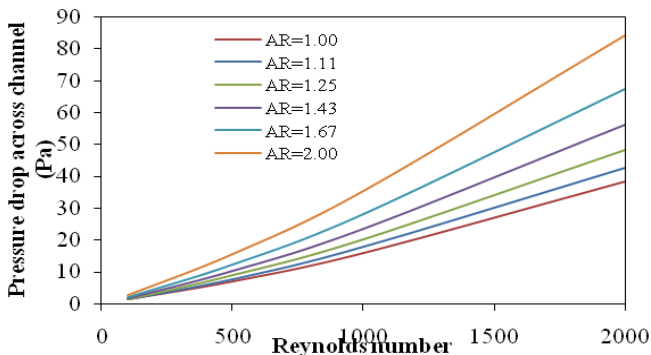


Figure 12. Duct pressure drop Variation with Reynolds number

Reynolds number (=500) and the slope value is altered when the Reynolds number is 2000. The variation of drop in fluid outlet temperature with Reynolds number is shown in Fig.11. The variation of compared with inlet temperature and there is a decrease in temperature drop with increasing Reynolds number. This indicates that the heat loss is less in the duct walls. The water-nanofluid shows an increase in temperature on the duct outlet. Likewise, temperature drop occurs with increasing duct aspect ratio. The variation over the duct pressure drop with the Reynolds number is shown in Fig.12. It is seen that increase in Reynolds number makes the pressure drop

to increase along its duct walls. The results of duct aspect ratio shows that there is an increase in pressure drop with increasing duct aspect ratio.

5. CONCLUSIONS

It is clear from the above analysis that when the aspect ratio of the duct increases, the drop in pressure increases. This is due to the fact that high valued Reynolds number inside the inlet duct. It is further found that temperature in nanofluid reduces with increased Reynolds number. This indicates heat loss through the duct is lesser in the duct walls. The pressure drop is high if the aspect ratio reduces and further the temperature across the channel increases and the temperature across the wall reduces. Further, the study can be carried out to analyse various nano-fluid mixtures to test its feasibility for better flow rate.

REFERENCES

- [1] Shah, R.K., Laminar flow forced convection in ducts: a source book for compact heat exchanger analytical data, Academic press, London, A.L., 2014.
- [2] Park, K.W. and Pak, H.Y., Numerical Heat Transfer: Part A: Applications, 41(1), 19 (2002).
- [3] Yang, Y., Zhang, Z.G., Grulke, E.A., Anderson, W.B. and Wu, G., International Journal of Heat and Mass Transfer, 48(6), 1107 (2005).
- [4] Akbarinia, A. and Behzadmehr, A., Applied Thermal Engineering, 27(8), 1327 (2007).
- [5] Vajjha, R.S. and Das, D.K., International Journal of Heat and Mass Transfer, 52(21), 4675 (2009).
- [6] Bianco, V., Chiacchio, F., Manca, O. and Nardini, S., Applied Thermal Engineering, 29(17), 3632 (2009).
- [7] Nassan, T.H., Heris, S.Z. and Noie, S.H., International Communications in Heat and Mass Transfer, 37(7), 924 (2010).
- [8] Huminic, G. and Huminic, A., Experimental Thermal and Fluid Science, 35(3), 550 (2011).
- [9] Paul, G., Chopkar, M., Manna, I. and Das, P.K., Renewable and Sustainable Energy Reviews, 14(7), 1913 (2010).
- [10] Mohammed, H.A., Al-Aswadi, A.A., Shuaib, N.H. and Saidur, R., Renewable and Sustainable Energy Reviews, 15(6), 2921 (2011).
- [11] Raveshi, M.R., Keshavarz, A., Mojarrad, M.S. and Amiri, S., Experimental Thermal and Fluid Science, 44, 805 (2013).
- [12] Peyghambarzadeh, S.M., Hashemabadi, S.H., Jamnani, M.S. and Hoseini, S.M., Applied Thermal Engineering, 31(10), 1833 (2011).
- [13] Kamyar, A., Saidur, R. and Hasanuzzaman, M., International Journal of Heat and Mass Transfer, 55(15), 4104 (2012).
- [14] Huminic, G. and Huminic, A., Renewable and Sustainable Energy Reviews, 16(8), 5625 (2012).
- [15] Suresh, S., Venkataraj, K.P., Selvakumar, P. and Chandrasekar, M., Experimental Thermal and Fluid Science, 39, 37 (2012).
- [16] Mohammed, H.A., Hasan, H.A. and Wahid, M.A., International Communications in Heat and Mass Transfer, 40, 36 (2013).